ENVIRONMENTAL RESEARCH
COMMUNICATIONS

LETTER • OPEN ACCESS

# The impact of the COVID-19 lockdown on greenhouse gases: a multi-city analysis of in situ atmospheric observations

To cite this article: V Monteiro *et al* 2022 *Environ. Res. Commun.* **4** 041004

Environmental Research Communications

LETTER

# The impact of the COVID-19 lockdown on greenhouse gases: a multi-city analysis of in situ atmospheric observations

V Monteiro[1], N L Miles[1], S J Richardson[1], J Turnbull[2,3], A Karion[4], J Kim[5], L Mitchell[6], J C Lin[6], M Sargent[7], S Wofsy[8], F Vogel[9] and K J Davis[1,10]

[1] Department of Meteorology and Atmospheric Science, The Pennsylvania State University, University Park, PA, United States of America
[2] National Isotope Centre, GNS Science, Lower Hutt, New Zealand
[3] CIRES, University of Colorado, Boulder, CO, United States of America
[4] National Institute of Standards and Technology, Gaithersburg, MD, United States of America
[5] Scripps Institution of Oceanography, University of California San Diego, San Diego, CA, United States of America
[6] Department of Atmospheric Sciences, University of Utah, Salt Lake City, UT, United States of America
[7] School of Engineering and Applied Sciences, Harvard University, Boston, MA, United States of America
[8] Department of Earth and Planetary Sciences, Harvard University, Boston, MA, United States of America
[9] Climate Research Division, Environment and Climate Change Canada, Toronto, ON, Canada
[10] Earth and Environmental Systems Institute, The Pennsylvania State University, University Park, PA, United States of America

**E-mail:** vanessa_monteiro@psu.edu

**OPEN ACCESS**

**RECEIVED**
17 January 2022

**REVISED**
8 April 2022

**ACCEPTED FOR PUBLICATION**
12 April 2022

**PUBLISHED**
27 April 2022



**Keywords:** covid-19 lockdown, greenhouse gas, emission reduction, North America, observational metrics

Supplementary material for this article is available online

## Abstract

We tested the capabilities of urban greenhouse gas (GHG) measurement networks to detect abrupt changes in emissions, such as those caused by the roughly 6-week COVID-19 lockdown in March 2020 using hourly *in situ* GHG mole fraction measurements from six North American cities. We compared observed changes in $CO_2$, CO, and $CH_4$ for different mole fraction metrics (diurnal amplitude, vertical gradients, enhancements, within-hour variances, and multi-gas enhancement ratios) during 2020 relative to previous years for three periods: pre-lockdown, lockdown, and ongoing recovery. The networks showed decreases in $CO_2$ and CO metrics during the lockdown period in all cities for all metrics, while changes in the $CH_4$ metrics were variable across cities and not statistically significant. Traffic decreases in 2020 were correlated with the changes in GHG metrics, whereas changes in meteorology and biology were not, implying that decreases in the $CO_2$ and CO metrics were related to reduced emissions from traffic and demonstrating the sensitivity of these tower networks to rapid changes in urban emissions. The enhancements showed signatures of the lockdowns more consistently than the three micrometeorological methods, possibly because the urban measurements are collected at relatively high altitudes to be sensitive to whole-city emissions. This suggests that urban observatories might benefit from a mixture of measurement altitudes to improve observational network sensitivity to both city-scale and more local fluxes.

## 1. Introduction

During 2020, the coronavirus (COVID-19) pandemic led to governments imposing restrictions, including those on travel, in efforts to reduce disease transmission. Traffic and economic activities decreased in many places around the globe, including in the U.S. and Canadá, in March 2020 [1–3]. Because urban systems account for the majority of anthropogenic greenhouse gas (GHG) emissions, the COVID-19 shutdown forced a large and rapid global-scale change in emissions. For example, the most recent Global Energy Review 2021 [4] reported a 5.8% decrease in global carbon dioxide ($CO_2$) emissions during 2020. Other studies [5] estimated an even larger reduction in global $CO_2$ emissions, approximately 9%, when comparing the first half of 2019 to the same period in 2020, and such a drop in emissions is synchronous with the changes in ground transportation [5, 6].

Cities experienced even larger decreases in GHG emissions during the first half of 2020. In Athens, Greece, pollutants related to traffic emissions decreased by 30% to 35% [7]. Representative cities of Canada, $CO_2$ emissions from vehicle fuel consumption decreased about 37% from March to April 2020, and April 2020 exhibited half of the estimated emissions of the same period in 2019 [2].

Despite the economic impacts and health outcomes, the COVID-19 pandemic presents a unique scientific opportunity to test the ability of GHG observing networks to detect rapid changes in emissions. Urban atmospheric measurement networks were designed to quantify GHG emissions. They aim to provide independent evaluation of GHG emissions mitigation efforts and to improve understanding of urban metabolism [8]. Such networks have been deployed for several years at several cities across the globe, have near-real-time dedicated high-precision, high-accuracy measurements of $CO_2$, carbon monoxide (CO), and methane ($CH_4$) [9–15]. These networks have been used to infer [16] or quantify [17] changes in emissions over time, and with atmospheric inverse systems for the quantification of urban emissions [12], [18–20]. Recently, this technique was used to quantify the relative reduction of $CO_2$ emissions from activities associated with COVID-19 in Los Angeles and D.C./Baltimore, [20] and San Francisco [21]. Both studies found emissions reductions on the order of 30%.

Atmospheric inversion techniques are complex systems that rely on accurate quantification and interpretation of urban GHG measurements. Local anthropogenic emissions of GHGs result in small increases in total mole fractions relative to the incoming background concentrations (urban 'enhancements' [22]). Quantifying the mole fraction enhancements due to urban anthropogenic emissions requires careful calibration of instruments [10], careful quantification of GHG background conditions [23–25] accurate modeling of atmospheric transport [26], and either accurate modeling of the biosphere [27] or the use of tracers of anthropogenic activity [28].

Further, atmospheric inversions take advantage of only a fraction of the information available in the observational GHG networks deployed in cities. Alternative observational metrics include micrometeorological quantities such as vertical gradients and variances [29], and tracer ratios that can factor out uncertainties caused by atmospheric transport. Some metrics, including the amplitude of the daily cycle of a GHG, are simple and can be quantified with a single observation site.

In this study, we evaluate observations from six multi-year urban GHG networks, five in the United States and one in Canada, during three periods in 2020 (pre-lockdown, lockdown, and the ongoing recovery period) defined by changes in traffic counts, relative to the same periods in previous years. We hypothesize that changes caused in traffic during the COVID-19 lockdown, which reduced emissions of GHG, can be identified in observational metrics derived from GHG mole fraction measurements from urban-scale GHG networks. Thus, our objectives are to test the ability of a range of observational metrics derived from $CO_2$, CO, and $CH_4$ measurements of dedicated GHG networks to detect short-term emission changes such as occurred during the lockdown and assess how these findings vary from city to city. Since the major source of fossil-fuel anthropogenic $CO_2$ emissions is on-road transportation (e.g., in Los Angeles it accounts for 43% [30]), we hypothesize that $CO_2$ emissions are affected by the COVID-19 lockdown due to the reduction of traffic activities within this period, and the observational metrics will be capable of detecting such changes. Similarly, we expect a decrease in CO observational metrics, which is a tracer for transport and is a coincident measurement with the GHG networks. $CH_4$, however, should not be affected by changes in traffic.

Our study does not quantify emissions. Rather, we examine the sensitivity of mole fraction observations to the changes in emissions caused by the lockdown. We show how the impact of the lockdown is reflected across five observational metrics, to test their ability to detect changes in emissions: amplitude of the diurnal cycle, vertical gradients, enhancements, variances, and multi-gas enhancement ratios. Except for enhancements, these observational approaches are not used in atmospheric inversion systems, thus, we are exploring new methods, and we are also illustrating the signature of the lockdown versus competing factors, such as weather and biological changes. Because there are possible confounders of changed atmospheric concentrations of GHG, such as meteorology and biology, we explore attribution by searching for correlations of our GHG metrics with indices related to changes in traffic, biological fluxes, here represented by the enhanced vegetation index (EVI), and atmospheric transport, here represented by ventilation factor (VF). Atmospheric inversion techniques require substantial additional effort, expertise, and resources beyond that required for atmospheric observations, and may not be always available. This paper examines how changes in emissions can be evaluated without requiring the infrastructure to perform an atmospheric inversion and provides a pathway for less well-resourced researchers (e.g., in developing countries) to assess emissions.

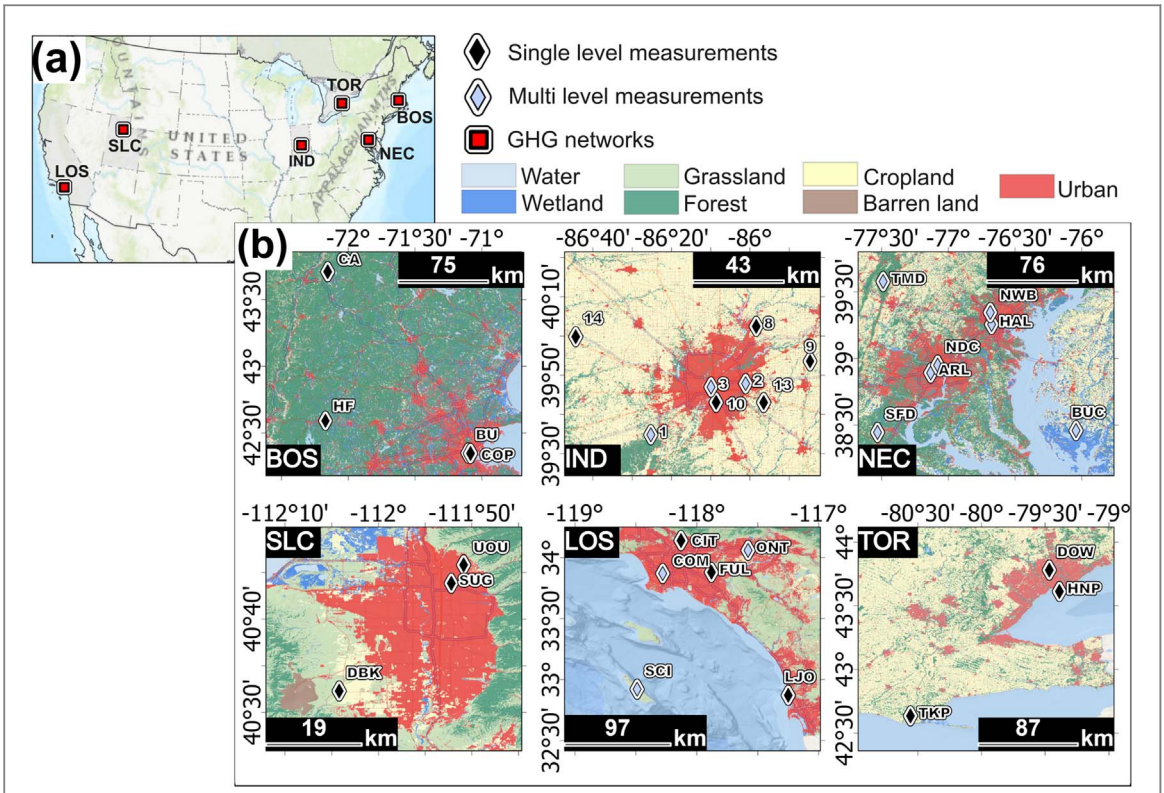


**Figure 1.** Urban greenhouse gas (GHG) networks locations in the U.S. and Canada. (a) Cities where the GHG networks are located. (b) The locations of measurement sites that were used in this study in each city. These sites represent a subset of each GHG network. The background map summarizes land cover types [32, 33], used to determine if a site is considered urban or rural. The description of each land cover category can be found in table S2 (available online at stacks.iop.org/ERC/4/041004/mmedia). Black symbols represent the sites where only single-level measurements are available, and blue symbols represent the sites where multi-level measurements are available.

## 2. Materials and Methods

### 2.1. Greenhouse gas networks

We analyzed greenhouse gas ($CO_2$, $CH_4$) and CO observations using a data synthesis product of observations from five networks across the U.S. and one in Canada [9–13], [31]. Herein, the networks are identified by the name of the cities where they are located (figure 1): Boston (Massachusetts; BOS), Northeast Corridor (Baltimore, Maryland, and Washington D.C.; NEC), Indianapolis (Indiana; IND), Salt Lake City (Utah; SLC), Los Angeles (California; LOS), and Toronto (Ontario; TOR).

The networks were designed to continuously measure $CO_2$ and $CH_4$ mole fractions, typically using Cavity Ring-Down Spectroscopy (CRDS), at multiple sites. In SLC, the instruments include a combination of analyzers based on non-dispersive infrared absorption and off-axis integrated cavity output spectroscopy [34]. The instruments were calibrated on WMO (World Meteorological Organization) scales, X2007 for $CO_2$, X2004A for $CH_4$, and X2014A for CO [10–13], [34, 35]. Inlets are installed on communication towers or on building tops. Multi-level measurements are available at specific sites/cities (LOS, IND, NEC) allowing for the assessment of GHG vertical profiles. The networks have been operating for several years, the earliest starting in SLC in 2001, and the newest starting in Toronto in 2016 (table S1 (available online at stacks.iop.org/ERC/4/041004/mmedia)). Some of them include continuous measurements of CO (BOS, IND, LOS, TOR). The data are obtained at high frequency and averaged hourly.

### 2.2. Site selection

Most of the influence of the $CO_2$ mole fraction enhancement at the Indianapolis towers was within 10 km of the tower location [25]. Since the boundary layer processes defining this influence area is unlikely to vary substantially from city to city, we used the 2016 U.S. National Land Cover Database (NLCD) [32] and 2015 land Cover of Canada [33] to define urban sites as those with at least 50% of urban land cover by area within a radius of 10 km, and rural sites as all sites with less than 50% of urban land cover (see Sub-classification at table S2 and figure S1 (available online at stacks.iop.org/ERC/4/041004/mmedia)).

### 2.3. Observational metrics

We searched for the signature of the lockdown in the GHG networks' observations using: 1) amplitude of the diurnal cycle, 2) vertical gradients, 3) enhancements above background, 4) temporal variances, 5) the enhancement ratio of $CO_2$ and $CH_4$ ($\Delta CO_2$:$\Delta CH_4$), and 6) the enhancement ratio of CO and $CH_4$ ($\Delta CO$:$\Delta CH_4$). Each metric is evaluated for sensitivity to the abrupt decrease in anthropogenic activities caused by COVID-19 restrictions.

The amplitude of the diurnal cycle is defined as the difference between the maximum and the minimum hourly-averaged mole fraction for each day, using local standard time (LST) to define the start and end of each day. Higher emissions should lead to larger diurnal cycles. The primary advantage of this metric is simplicity; this can be computed at any individual measurement site. It is difficult to use to quantify emissions, and the influence area is not well-known.

Vertical gradients are micrometeorological metrics that are quantitatively linked to local emissions via flux-gradient relationships in the surface layer [36] and convective boundary layer [37, 38]. The influence area or flux footprint for this metric is typically 1 $km^2$ or less, similar to an eddy covariance flux footprint [39, 40]. The relatively small footprint makes this metric sensitive to local emissions. We compute vertical gradients at the multi-level sites located in IND, NEC, and LOS, using the highest and lowest inlets on the towers.

Temporal variance in mole fractions is another micrometeorological metric that is quantitatively linked to local emissions via flux-variance relationships in the surface layer [29] and convective boundary layer [41]. This metric has similar characteristics to vertical gradients, but with the important simplification that only one measurement level is necessary. Within-hour temporal variances in mole fractions are computed from the highest-frequency data available from the observing sites.

Enhancements [22] are defined as the difference between the city background (see text S1(available online at stacks.iop.org/ERC/4/041004/mmedia)) and the mole fraction observed at each urban site. Enhancements reflect regional emissions changes. The sensitivity of this metric to regional emissions makes this metric the typical input for urban inverse flux estimates [18]. Enhancements are influenced by biological and anthropogenic fluxes, and by variability in atmospheric transport.

Enhancement ratios are intended to eliminate sensitivity to atmospheric transport by studying the change in one trace gas enhancement relative to another trace gas enhancement. This metric is determined by the slope of the relationship between two gases' enhancements, using a York fit [42]. In this study we use $CH_4$ as a normalizing factor, hypothesizing that $CH_4$ emissions may not have been strongly impacted by the lockdown.

Since the inlet heights vary by site (table S1 (available online at stacks.iop.org/ERC/4/041004/mmedia)), we used the highest level of measurement at each site for all the metrics, except for the vertical gradients, which require multiple levels. For each metric a decrease is consistent with a decrease in emissions. Additional details about the metrics are found in text S1 (available online at stacks.iop.org/ERC/4/041004/mmedia).

### 2.4. Periods of study, data selection, and interannual analysis

We computed the observational metrics for $CO_2$, as well as CO and $CH_4$ at the cities where these measurements were available, during three periods of time and across multiple years of observations. We defined a pre-lockdown phase from 07 February to 14 March, a lockdown phase from 21 March to 14 May, and an ongoing recovery phase from 15 May to 15 June. We used the changes in driving navigation requests since 13 January 2020 from the Apple Mobility Trends Reports [43] as a consistent reference across the six cities for the definition of these periods. The pre-lockdown represents high and presumably typical traffic patterns; the lockdown represents a period when traffic intensity was consistently low; and the recovery phase represents a period when traffic intensity steadily increased (figure S2 (available online at stacks.iop.org/ERC/4/041004/mmedia)).

All the urban networks maintain long-term measurements, but instrument failures and calibration issues result in occasional data loss. For our analyses, we limited the number of years from 2 to 6 years prior to 2020, and only used the measurement site-years when more than 30% of data are available for the site within each period of study. Thus, the number of sites used at a given city was kept constant across years, and years were chosen to enable a multi-year record with a maximum number of sites for each city (see table S3 (available online at stacks.iop.org/ERC/4/041004/mmedia) for sites and years included).

We used long-term records and focused on interannual variability to minimize the impact that temporal variability in atmospheric transport and biological fluxes would have on observational metrics. Boundary layer depths and winds, and biological $CO_2$ and $CH_4$ fluxes strongly vary with time of year. A direct comparison of pre-lockdown, lockdown, and recovery time periods within the year 2020 alone would be confounded by these seasonal changes. Instead, we computed the relative percent changes ($P_{change}$) in observational metrics across multiple years for the three time periods. For example, during the lockdown, for each urban site ($s$), we compared the average over time, denoted by the overbar ($\bar{M}$), of a given metric ($M$) in 2020 to the same metric computed at the same time for each year ($i$), but averaged over all the available previous years ($y$); and then, we average the relative percent change for each city, using all the city's urban sites ($N$),

$$P_{change} = \frac{1}{N}\sum_{N}^{s=1}\left(100 \cdot \frac{\bar{M} - \frac{1}{y}\sum_{i=1}^{y}\overline{M_i}}{\frac{1}{y}\sum_{i=1}^{y}\overline{M_i}}\right)_s \quad (1)$$

and similarly for both the pre-lockdown and ongoing recovery periods. For vertical gradients and within-hour variances, we averaged over morning hours, defined herein as 06:00 to 11:59 LST and late afternoon hours, 16:00 to 19:59 LST, when traffic emissions are expected to be relatively large and atmospheric mixing is relatively weak leading potentially to large vertical gradients. For enhancements and enhancement ratios, we used afternoon averages, 12:00 to 16:59 LST, when the atmospheric boundary layer is most likely well mixed, a typical approach used in atmospheric inversions. Figure S3 (available online at stacks.iop.org/ERC/4/041004/mmedia) demonstrates the procedure for one of the sites.

### 2.5. Ancillary measurements

Changes in the trace gas mole fractions measured at towers occur not only due to changes in anthropogenic fluxes (e.g., changes in the transportation sector, electricity production), but also due to changing biological fluxes and changing atmospheric conditions (such as atmospheric boundary layer depth and wind speed). The lockdown in March 2020 happened concurrently with the transition of the seasons and lasted roughly for two months. Thus, to support the interpretation of changes in the observational metrics, we explored the changes in measurements indicative of meteorological and biological influences. We used the same methodology described by equation (1) to assess changes in traffic, using traffic datasets obtained from local and federal agencies. Similarly, we computed changes in the ventilation factor (VF) using boundary layer depth and wind speed obtained from North American Regional Reanalysis (NARR)[44] , to assess changes in meteorology, and enhanced vegetation index (EVI), obtained from satellite observations [45, 46], to assess changes in biological activity. See text S3 (available online at stacks.iop.org/ERC/4/041004/mmedia) for a detailed description of the methodology.

We also assessed the metrics at the rural sites for each network as an alternative test for changes due to biology. If these sites had no anthropogenic emissions within the footprint of the measurements, we could isolate the biological signal using three of the five metrics (amplitude of the diurnal cycle, vertical gradients, and variances). We can not use the enhancement metric since the background is determined from rural sites, thus no enhancement nor enhancement ratios can be obtained at these sites. To match the same periods of time in rural and urban sites' measurements and use the same sites within cities across the metrics (see table S3 (available online at stacks.iop.org/ERC/4/041004/mmedia)), we compared only 2019 and 2020.

## 3. Results and discussion

### 3.1. Carbon dioxide and carbon monoxide metric changes during the lockdown

The prevailing pattern in all the cities was that during the lockdown, the networks detected a reduction in 2020 relative to preceding years in all the observational metrics for $CO_2$ and CO (figures 2(a), (b)). Regarding $CO_2$, the amplitude of the diurnal cycle decreased between 7.2% (NEC) and 28.9% (BOS); vertical gradients decreased 58% (IND); enhancements decreased 18.2% (LOS) to 122.7% (SLC); variances decreased 28.3% (LOS) to 62.4% (BOS); all suggesting declines in emissions of $CO_2$ during the lockdown period in 2020. The $\Delta CO_2$:$\Delta CH_4$ ratio also decreased 32% (IND), which would also suggest a decline of $CO_2$ if $CH_4$ emissions remained constant. All the above relative differences were statistically significant (95% confidence level; refer to details in text S2 (available online at stacks.iop.org/ERC/4/041004/mmedia)), suggesting a decrease in $CO_2$ emissions in all the cities. There was only one occasion when the percent relative change in the metric was positive (3.7%) and statistically significant: the amplitude of the diurnal cycle in LOS. For CO relative changes, results also indicate significant declines in 2020 for all metrics for all cities where it is measured, consistent with the reduced traffic levels and CO emissions during the lockdown period (see section 3.3). The largest decrease in CO was observed in BOS enhancements, 96.3%, and the smallest one in the enhancements in TOR, 2.4%, both results statistically significant. It is noticible that CO metrics were also smaller in 2020 than in previous years even before the lockdown event. It can be explained because the global signature of CO concentration has decreased over the last several decades [47].

Most of the $CO_2$ metric changes in the pre-lockdown were not statistically significant, suggesting no significant changes in emissions for 2020 relative to previous years. The ongoing recovery period, however, showed statistically significant changes for 2020 relative to previous years. For most cases the relative changes were negative, suggesting that $CO_2$ emissions in 2020 were lower than previous years (figure S4 (available online at stacks.iop.org/ERC/4/041004/mmedia)). The amplitude of the diurnal cycle of $CO_2$ in LOS and TOR increased in 2020 by 37.9% and 60.7%, respectively, in contrast to the enhancements at these cities that

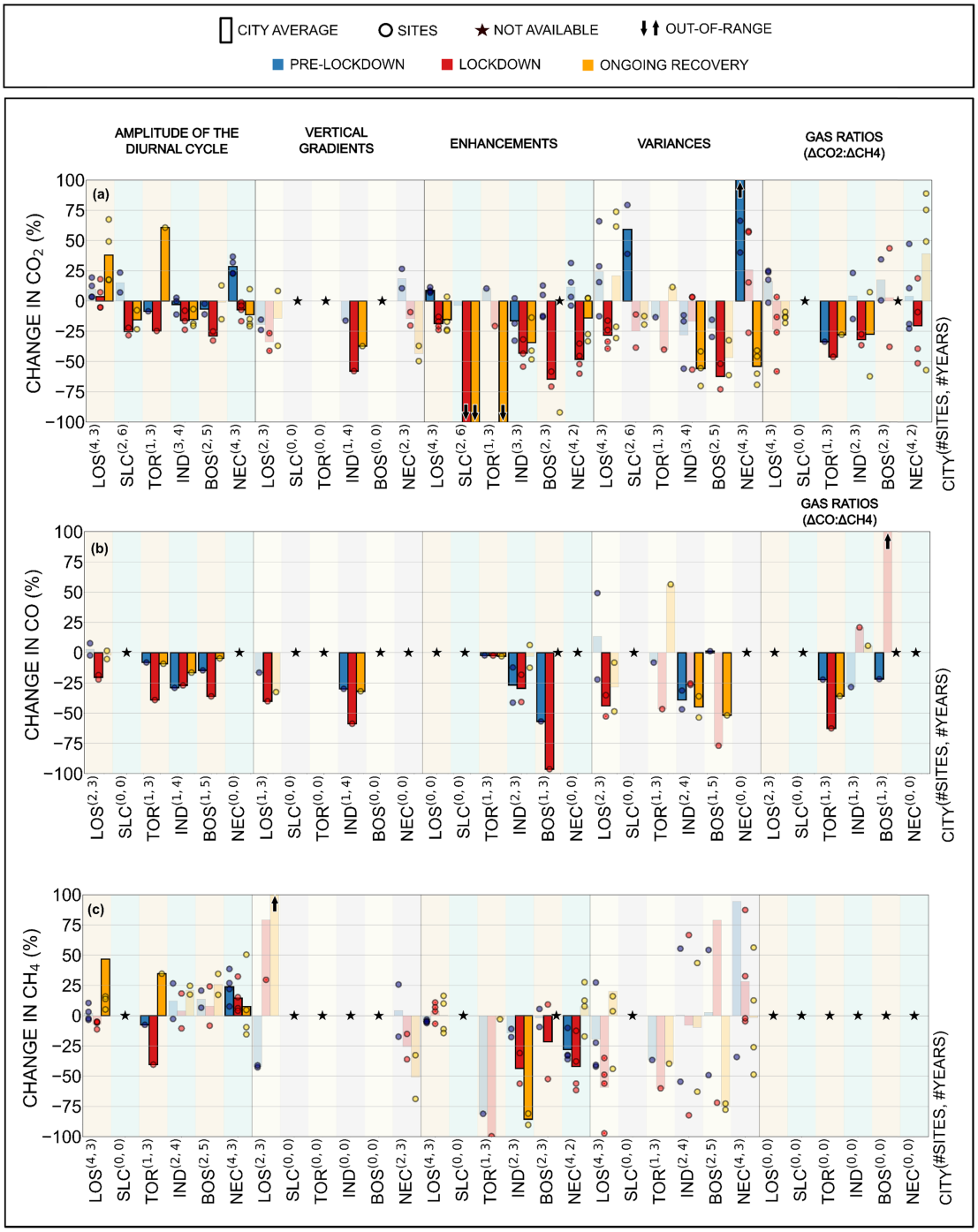


**Figure 2.** Greenhouse gas ($CO_2$, $CH_4$) and CO metrics percent change from 2020 relative to past years of mole fraction records (computed by equation 1) for five observational metrics (described in section 2.3): amplitude of the diurnal cycle, vertical gradients, mole fraction enhancements, variances within the hour, and enhancement ratios. (a) Percent relative change of $CO_2$ mole fraction metrics. (b) Percent relative change of CO mole fraction metrics. (c) Percent relative change of $CH_4$ mole fraction metrics. Colored bars represent the average of the sites within the city, circles represent individual site changes that compose the city average, stars show there was no data available for that metric or evaluated period. Cities are represented by their initials followed by the number of sites and the number of years previous to 2020 included in the analysis. Lighter colors represent results not statistically significant (95% confidence level). The statistically significant percent changes that extend out-of-scale are: $CO_2$ enhancement in SLC during lockdown, −122.7%, and during ongoing recovery, −125.7%; $CO_2$ enhancement in TOR during ongoing recovery, −347.7%; $CO_2$ variances in NEC during pre-lockdown, 124.1%.

decreased within the same period. Overall, these results suggest a drop in $CO_2$ and CO emissions in 2020 across all cities during the lockdown relative to previous years, and no such coherent change in emissions in 2020 relative to previous years prior to the lockdown. The recovery period results, while less consistent, may be consistent with reduced emissions in 2020 relative to prior years.

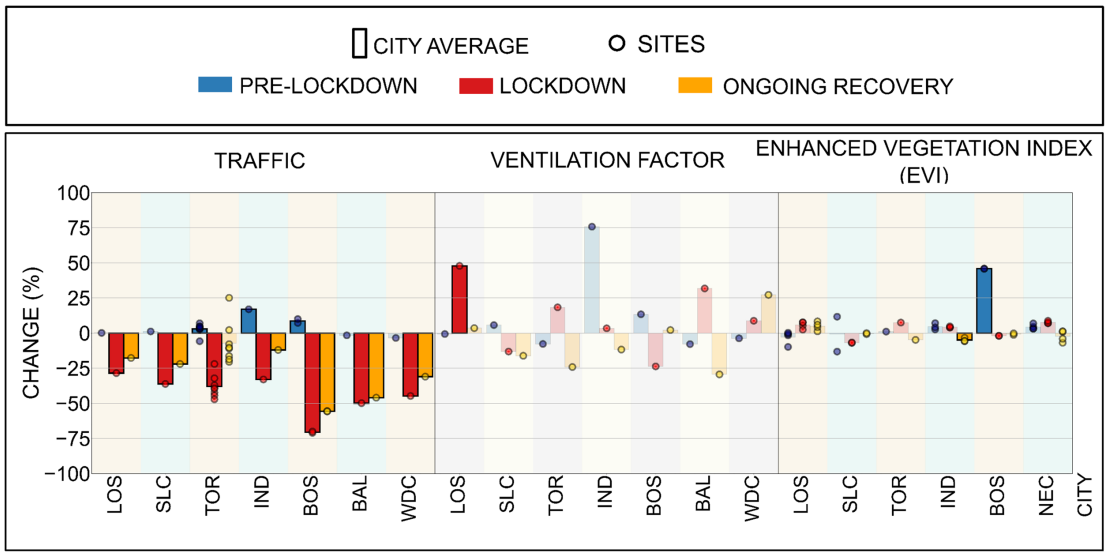


**Figure 3.** Relative percent change in ancillary measurements from 2020 relative to previous years: traffic, ventilation factor (VF), and enhanced vegetation index (EVI), calculated as described in section 2.5 and supporting information text S3 (available online at stacks.iop.org/ERC/4/041004/mmedia). For traffic and VF, NEC was split in BAL (Baltimore) and WDC (Washington, D.C.). The specifics of the traffic data vary among the cities. Whereas in LOS the data shown here represents vehicle miles travelled, the other cities have volume counts (see table S5 (available online at stacks.iop.org/ERC/4/041004/mmedia)). Lighter colors represent results that are not statistically significant (95% confidence level).

### 3.2. Methane changes in 2020

Contrary to the significant, consistent changes in $CO_2$ and CO across cities, the signs of changes in the metrics for methane ($CH_4$) during the lockdown varied across cities and were not usually statistically significant (figure 2(c)) and vary in sign within each city. TOR had a significant decrease (40.5%) in the amplitude of the diurnal cycle of methane, but for all the other metrics in TOR, the decrease was not statistically significant. In NEC, two metrics were statistically significant during the lockdown period, but disagreed in the sign of change; the amplitude of the diurnal cycle was 14.5% larger in 2020 than in previous years, but enhancements were 42% smaller in the same period. Similar inconsistent results describe the pre-lockdown and recovery periods. Thus, for all cities, and in any of the three periods studied, there are significant changes or contradictory results across metrics for $CH_4$. These variable and insignificant changes in metrics suggest no coherent changes in 2020 methane emissions relative to previous years. Urban anthropogenic $CH_4$ emissions come primarily from leaks in the natural gas distribution system, landfills, and wastewater treatment facilities [48]. These sources are unlikely to be altered by the lockdown, so this result is expected.

### 3.3. Traffic, meteorology, and biology

During the lockdown period, changes in traffic relative to previous years were statistically significant for all cities, whereas the changes in VF and EVI were smaller and not statistically significant (figure 3).

Traffic in 2020 tended to be high in the pre-lockdown, but during the lockdown, all cities showed a consistent drop in traffic ranging from 28.5% (LOS) to 70.6% (BOS). Even during the recovery period, traffic levels in 2020 were decreased compared to previous (from −12% in IND to −55.6% in BOS) across all cities.

In contrast to the persistent pattern in traffic, the 2020 changes in VF and EVI varied from city to city during the lockdown and were statistically insignificant. The random nature of changes in 2020 VF and EVI, contrary to the significant decreases in 2020 traffic levels, support the conclusion that the changes in $CO_2$ and CO observational metrics during the lockdown are consistent with decline in anthropogenic emissions during this period.

Furthermore, statistically significant correlations across cities were found between relative changes in $CO_2$ and CO metrics and traffic, but not between $CH_4$ metrics and traffic (table S4 (available online at stacks.iop.org/ERC/4/041004/mmedia)). For CO, the strongest significant correlation is between changes in traffic and vertical gradients ($r = 0.73$), followed by traffic and variances ($r = 0.62$). For $CO_2$, traffic changes were correlated with the amplitude of the diurnal cycle ($r = 0.44$) and the within-hour variances ($r = 0.43$). Significant correlations were not found between changes in any of the metrics and EVI or VF.

### 3.4. What can we learn from rural sites surrounding the cities?

Figure S5 (available online at stacks.iop.org/ERC/4/041004/mmedia) shows $CO_2$ observational metrics and EVI for both urban and rural sites. The relative percent changes in 2020 GHG metrics have similar magnitudes during the lockdown at both urban and rural sites and are, in most cases, statistically significant. The EVI changes are variable across cities and not statistically significant. Even rural sites have some urban landcover (figure S1 (available online at stacks.iop.org/ERC/4/041004/mmedia)). We hypothesize, therefore, that even the rural sites were sensitive to the decrease in traffic caused by the lockdown.

### 3.5. Sensitivity of metrics to emissions changes

The micrometeorological metrics (i.e., variances and vertical gradients) are sensitive to sampling altitude. The $CO_2$ and CO variances and vertical gradients did not consistently show statistically significant decreases during the lockdown, whereas more integrative metrics, as the amplitude of the diurnal cycle and enhancements, showed more significant decreases (figure 2). Only IND with a 10 m AGL inlet, the lowest inlet among the cities with vertical gradients, shows a significant change in $CO_2$. Figure S6 (available online at stacks.iop.org/ERC/4/041004/mmedia) shows results for all metrics when computed with lower altitude measurements. Variances showed increased significance in IND when the 10 m inlet was used. LOS and NEC, whose lower altitude inlets are between 25 and 50 m AGL, did not show as clear increase in variance at lower altitudes. The amplitude of diurnal cycle and enhancements were not strongly influenced by changing the sampling altitude. We conclude that micrometeorological metrics are more sensitive when lower altitude measurements are available.

The lack of significant changes in the enhancement ratios (figure 2) is surprising. We hypothesize that, rather than eliminating variability introduced by year-to-year changes in VF, that this ratio introduced variability caused by $CH_4$ emissions, confounding the clear decreases in $CO_2$ and CO enhancements.

The figure S7 (available online at stacks.iop.org/ERC/4/041004/mmedia) shows the results of the analysis for some observational metrics when comparing 2019 to previous years of measurements and excluding 2020. The most relevant difference from these results and the results presented in figure 2 are for the lockdown period. While in figure 2 there is a consistent and coherent decrease in the observational metrics, for 2019 versus previous years, evaluated for the same timeframe, there is not a consistent pattern. Carbon monoxide has very few statistically significant results for 2019 compared to previous years, and most of them are in the period before the period equivalent to the lockdown. For $CO_2$, there is more variability in the percent changes for 2019 versus other years than for 2020 versus other years. There are fewer statistically significant results in 2019, while in 2020 the metrics captured a decrease in all metrics (for both $CO_2$ and CO). $CH_4$ did not show a clear pattern for either year's comparisons.

## 4. Conclusions

Long-term *in situ* GHG networks show great potential for detecting temporal changes in urban GHG emissions. Using observational metrics, all six *in situ* networks found evidence consistent with reduced anthropogenic emissions of $CO_2$ and CO caused by reduced traffic during the COVID-19 lockdown, and not associated with changes in biology or meteorology. Pre-lockdown and ongoing recovery periods had more variable metric changes, most of which were not statistically significant. Also, only traffic showed significant changes in 2020 relative to previous years. Not all the metrics showed a statistically significant decrease during the 2020 lockdown, highlighting the complicated relationship between biological, meteorological, and anthropogenic processes for $CO_2$.

Comparing 2019 (when no abrupt changes in GHG observational metrics were expected) with previous years showed a random pattern, as opposed to the more consistent signal observed for 2020 compared to previous years. This result indicates that, even though some metrics did not present a statistically significant result during the 2020 lockdown, the reduction in GHG emissions during this period was captured.

Of the observational metrics analysed in this study, the amplitude of the diurnal cycle and the enhancements were the metrics that more robustly detected statistically significant results during the lockdown. Enhancements, were the metric that is most sensitive to abrupt changes, with the largest percent relative changes of the metrics. This result is encouraging as these networks support atmospheric inversion systems that are based on the enhancements. The consistency of these results across cities with exceedingly different background conditions, urban geometries, and geographic and biological settings yields strong evidence of the effectiveness of the *in situ* observing networks.

Our analyses suggest that *in situ* GHG networks can be enhanced by multi-level measurements, particularly low altitude measurements, and multiple gas observations. Low altitude (10 m AGL) observations from IND showed significant detection of changes in GHG emissions using both vertical gradient and variances. It is preferable to combine the low-altitude measurements with a top level inlet installed high enough to capture the

vertical profile, as in IND, where the top inlet is at $>$ 50 m AGL. These low altitude measurements and micrometeorological metrics are more sensitive to local emissions changes, complementing the enhancements that are sensitive to city-wide emissions changes. Furthermore, our ability to compare across $CO_2$, CO and $CH_4$ strengthened our ability to attribute observed changes. We were able to confirm that changes in $CH_4$ were not statistically significant over the period studied, ruling out a strictly meteorological cause of the changes in $CO_2$ metrics. The correspondence between $CO_2$ and CO further strengthened the case for attributing the changes in $CO_2$ to changes in traffic.

Finally, we emphasize the power of sustained observations. The short-term changes in GHG emissions would be more difficult to detect if long-term measurements were not available.

## Acknowledgments

We acknowledge the ongoing contributions of C. Miller, R. Weiss, and R. Keeling, Principal Investigators of the Los Angeles greenhouse gas network, and D. Worthy and ECCC's GGML for their tireless efforts in maintaining Canada's and Los Angeles's GHG atmospheric GHG monitoring programs, respectively. We also thank S. Prinzivalli, M. Stock, C. Fain, C. Draper, S. Baldelli, and E. DiGangi (Earth Networks, Inc.) for LOS, NEC, and BOS (CA site only) tower maintenance and data processing. We acknowledge the efforts of R. Bares, B. Fasoli, and M. Garcia in maintaining the Salt Lake City network, and E. Gottlieb and J. Budney for Boston network maintenance and data processing as well.

These analyses were supported by NIST, Grant 70NANB10H245 and NOAA's AC4 program, Grant NA21OAR4310227 to Pennsylvania State University, NIST Grant 70NANB19H130 to Scripps Institution of Oceanography, NOAA Grant NA17OAR4310084 to the University of Utah, NOAA Grants NA17OAR4310086 and NA20OAR4310303 to Harvard University.

The authors thank B. Haupt (The Pennsylvania State University), D. K. Martins (FLIR, Inc.), S. Miller (The Pennsylvania State University), B. Michalak (Earth Networks, Inc.) for assistance with INFLUX tower maintenance and data processing. The INFLUX (Indianapolis) network is supported by the National Institute of Standards and Technology (Project 70NANB10H245) and the National Oceanic and Atmospheric Administration (Award NA13OAR4310076).

The authors thank S. Murphy (The Pennsylvania State University) for assistance with Enhanced Vegetation Index (EVI) datasets, L. Zhang (The Pennsylvania State University) for assistance with meteorological reanalysis datasets, K. Verhulst (Jet Propulsion Laboratory) for assistance with LOS network background, and D. Allen and K. Mueller (NIST) for revisions and inputs.

## Data availability statement

The data that support the findings of this study are openly available at the following URL/DOI: https://doi.org/10.3334/ORNLDAAC/1743 (TOR, SLC, BOS), https://doi.org/10.18434/M32126 (NEC), https://doi.org/10.18434/mds2-2388 (LOS), and https://doi.org/10.18113/D37G6P (IND).

## ORCID iDs

V Monteiro https://orcid.org/0000-0002-9422-5635
J Kim https://orcid.org/0000-0002-2610-4882
L Mitchell https://orcid.org/0000-0002-8749-954X
K J Davis https://orcid.org/0000-0002-1992-8381

## References

[1] Parr S, Wolshon B, Renne J, Murray-Tuite P and Kim K 2020 Traffic Impacts of the COVID-19 Pandemic: Statewide Analysis of Social Separation and Activity Restriction *nat. Hazard. Rev.* **21** 04020025-1–04020025-10 (https://ascelibrary.org/doi/10.1061/%28ASCE%29NH.1527-6996.0000409)

[2] Tian X, An C, Chen Z and Tian Z 2021 Assessing the impact of COVID-19 pandemic on urban transportation and air quality in Canada *Sci. Total Environ.* **765** 144270

[3] Sahraei MA, Kuşkapan E and Çodur MY 2021 Public transit usage and air quality index during the COVID-19 lockdown *J. Environ. Manage.* **286** 112166

[4] IEA 2021 *Global Energy Review 2021.* (Paris: IEA) Accessed 1 July 2021. Retrieved from: (https://iea.org/reports/global-energy-review-2021)

[5] Liu Z *et al* 2020 Near-real-time monitoring of global $CO_2$ emissions reveals the effects of the COVID-19 pandemic *Nat. Commun.* **11** 1–12

[6] Le Quéré C *et al* 2020 Temporary reduction in daily global CO2 emissions during the COVID-19 forced confinement *Nat. Clim. Change* **10** 647–53
[7] Grivas G *et al* 2020 Integrating *in situ* Measurements and City Scale Modelling to Assess the COVID–19 Lockdown Effects on Emissions and Air Quality in Athens, Greece *Atmosphere* **11** 1174
[8] Davis KJ *et al* 2017 The Indianapolis Flux Experiment (INFLUX): A test-bed for developing urban greenhouse gas emission measurements *Elementa: Science of the Anthropocene* **5** 21
[9] Lin JC *et al* 2018 $CO_2$ and carbon emissions from cities: linkages to air quality, socioeconomic activity and stakeholders in the Salt Lake City urban area *Bull. Am. Meteorol. Soc.* **99** 2325–39
[10] Richardson SJ *et al* 2017 Tower measurement network of *in situ* $CO_2$, $CH_4$, and CO in support of the indianapolis FLUX (INFLUX) experiment *Elementa: Science of the Anthropocene* **5** 1–14
[11] Karion A *et al* 2020 Greenhouse gas observations from the northeast corridor tower network *Earth System Science Data* **12** 699–717
[12] Sargent M *et al* 2018 Anthropogenic and biogenic $CO_2$ fluxes in the Boston urban region *PNAS* **115** 7491–6
[13] Verhulst KR *et al* 2017 Carbon dioxide and methane measurements from the Los Angeles Megacity Carbon Project - Part 1: Calibration, urban enhancements, and uncertainty estimates *Atmos. Chem. Phys.* **17** 8313–41
[14] Vogel FR, Ishizawa M, Chan E, Chan D, Hammer S, Levin I and Worthy DEJ 2012 Regional non-$CO_2$ greenhouse gas fluxes inferred from atmospheric measurements in Ontario, Canada *Journal of Integrative Environmental Sciences,* **9** 41–55
[15] Pugliese SC *et al* 2018 High-resolution quantification of atmospheric $CO_2$ mixing ratios in the Greater Toronto Area, Canada *Atmos. Chem. Phys.* **18** 3387–401
[16] Mitchell LE *et al* 2018 Long-term urban carbon dioxide observations reveal spatial and temporal dynamics related to urban characteristics and growth *Proc. Natl Acad. Sci.* **115** 2912–7
[17] Lauvaux T *et al* 2013 Urban emissions of $CO_2$ from davos, switzerland: the first real-time monitoring system using an atmospheric inversion technique *Journal of Applied Meteorology and Climatology* **52** 2654–68
[18] Lauvaux T *et al* 2020 Policy-relevant assessment of urban $CO_2$ emissions *Environmental Science & Technology* **54** 10237–45
[19] Yadav V *et al* 2019 Spatio-temporally resolved methane fluxes from the Los Angeles Megacity *Journal of Geophysical Research: Atmospheres* **124** 5131–48
[20] Yadav V *et al* 2021 The impact of COVID-19 on $CO_2$ emissions in the Los Angeles and Washington DC/Baltimore metropolitan areas. *Geophys. Res. Lett.* **48** e2021GL092744
[21] Turner AJ *et al* 2020 Observed impacts of COVID-19 on urban $CO_2$ emissions. *Geophys. Res. Lett.* **47** e2020GL090037
[22] Miles NL *et al* 2017 Quantification of urban atmospheric boundary layer greenhouse gas dry mole fraction enhancements in the dormant season: results from the indianapolis flux experiment (INFLUX) *Elementa: Science of the Anthropocene* **5** 27
[23] Balashov NV, Davis KJ, Miles NL, Lauvaux T, Richardson SJ, Barkley ZR and Bonin TA 2020 Background heterogeneity and other uncertainties in estimating urban methane flux: results from the indianapolis flux experiment (INFLUX) *Atmos. Chem. Phys.* **20** 4545–59
[24] Karion A *et al* 2021 Background conditions for an urban greenhouse gas network in the Washington, DC, and baltimore metropolitan region *Atmos. Chem. Phys.* **21** 6257–73
[25] Miles NL *et al* 2021 The influence of near-field fluxes on seasonal carbon dioxide enhancements: results from the indianapolis flux experiment (INFLUX) *Carbon Balance Manage.* **16** 1–15
[26] Deng A *et al* 2017 Toward reduced transport errors in a high resolution urban $CO_2$ inversion system *Elementa: Science of the Anthropocene* **20** 5 (http://doi.org/10.1525/elementa.133)
[27] Wu K, Lauvaux T, Davis KJ, Deng A, Coto IL, Gurney KR and Patarasuk R 2018 Joint inverse estimation of fossil fuel and biogenic $CO_2$ fluxes in an urban environment: An observing system simulation experiment to assess the impact of multiple uncertainties *Elementa: Science of the Anthropocene* **17** 6 (http://doi.org/10.1525/elementa.138)
[28] Turnbull JC *et al* 2015 Toward quantification and source sector identification of fossil fuel $CO_2$ emissions from an urban area: Results from the INFLUX experiment *Journal of Geophysical Research: Atmospheres* **120** 292–312
[29] Kaimal JC and Finnigan JJ 1994 *Atmospheric Boundary Layer Flows: Their Structure And Measurement.* (New York: Oxford university press)
[30] Gurney KR *et al* 2019 The hestia fossil fuel $CO_2$ emissions data product for the Los Angeles megacity (Hestia-LA) *Earth System Science Data* **11** 1309–35
[31] Mitchell LE *et al* (in review) *A multi-city urban atmospheric greenhouse gas measurement data synthesis.*
[32] MRLC 2016 *Multi-Resolution Land Characteristics Consortium: 2016 National Land Cover Database (NLCD)* Accessed 02 August 2021Retrieved from: (https://arcgis.com/home/item.html?id=3ccf118ed80748909eb85c6d262b426f)
[33] Latifovic R 2019 *2015 Land Cover of Canada. Accessed 02 August 2021*Retrieved from(https://open.canada.ca/data/en/dataset/4e615eae-b90c-420b-adee-2ca35896caf6)
[34] Bares R *et al* 2019 The utah urban carbon dioxide (UUCON) and Uintah basin greenhouse gas networks: instrumentation, data, and measurement uncertainty *Earth System Science Data* **11** 1291–308
[35] Worthy DEJ 2003 Canadian baseline program: summer of progress to 2002 *Environment Canada, Meteorological Service of Canada*
[36] Dyer AJ 1974 A review of flux-profile relations *Boundary Layer Meteorology* **1** 363- 372
[37] Wyngaard JC and Brost RA 1984 Top-down and bottom-up diffusion of a scalar in the convective boundary layer *Journal of Atmospheric Sciences* **41** 102–12
[38] Patton EG, Sullivan PP and Davis KJ 2003 The influence of a forest canopy on top-down and bottom-up diffusion in the planetary boundary layer *Q. J. R. Meteorolog. Soc.* **129** 1415–34
[39] Weil JC and Horst TW 1992 Footprint estimates for atmospheric flux measurements in the convective boundary layer *Precipitation Scavenging and Atmosphere-Surface Exchange.* Vol. 2 ed SE Schwartz and WGN Slinn 717–28(Washington, D.C: Hemisphere Publishing)
[40] Horst TW 1999 The footprint for estimation of atmosphere-surface exchange fluxes by profile techniques *Boundary Layer Meteorol.* **90** 171–88
[41] Moeng CH and Wyngaard JC 1984 Statistics of conservative scalars in the convective boundary layer *Journal of Atmospheric Sciences* **41** 3161–9
[42] Cantrell CA 2008 Review of methods for linear least-squares fitting of data and application to atmospheric chemistry problems *Atmos. Chem. Phys.* **8** 5477–87
[43] 2020 Apple . Mobility Trends Reports. Accessed 1 July 2020. Retrieved from: (https://apple.com/covid19/mobility)
[44] Mesinger F *et al* 2006 North American regional reanalysis *Bull. Am. Meteorol. Soc.* **87** 343–60

[45] AppEEARS Team 2021 Application for Extracting and Exploring Analysis Ready Samples (AppEEARS). Ver. 2.61. NASA EOSDIS Land Processes Distributed Active Archive Center (LP DAAC), USGS/Earth Resources Observation and Science (EROS) Center, Sioux Falls, South Dakota, USA. Accessed 25 June 2021. Retrieved from: (https://lpdaacsvc.cr.usgs.gov/appeears)
[46] Didan K 2015 MOD13A2 MODIS/Terra Vegetation Indices 16-Day L3 Global 1km SIN Grid V006. NASA EOSDIS Land Processes DAAC. Accessed 1 July 2021. Retrieved from:
[47] Global Climate Change 2015 Fourteen years of carbon monoxide from MOPITT. Accessed 13 March 2022. Retrieved from: (https://climate.nasa.gov/news/2291/fourteen-years-of-carbon-monoxide-from-mopitt/)
[48] Lamb BK *et al* 2016 Direct and indirect measurements and modeling of methane emissions in indianapolis, indiana *Environmental Science & Technology* **50** 8910–7